ARTICLE NO. 78-1214R

Measurements of Flowfield Properties in a Gasdynamic Laser Nozzle Wake

C. W. Peterson*
Sandia Laboratories, Albuquerque, N. Mex.

Detailed measurements were made in the nonreacting (cold-flow) wake of a gasdynamic laser (GDL) nozzle array to provide flowfield data with which to evaluate theoretical GDL fluid mechanical models and numerical prediction schemes. Pitot pressure, stagnation temperature, and static pressure measurements were made across the wake and along the wake centerline at twelve streamwise locations and at two nozzle Reynolds numbers. Redundant static pressure measurements were made to identify and correct any probe interference errors caused by the small dimensional wake scales. Pitot measurements across the GDL nozzle boundary layer were included to provide information on the initial conditions to the wake, and hot wires were used to identify the regions of the wake where turbulence exists. Measured wake centerline static pressures were observed to be as much as 40% higher than wake edge static pressures. Turbulent wake centerline data and lateral wake profiles showed good agreement with predictions from an existing linearized similarity theory for turbulent GDL wakes. Measurements in a transitional wake indicated that transition begins near the wake edge and moves toward the wake centerline as Reynolds number is increased. Centerline flow properties observed in the transitional wake could not be predicted by transitional linearized similarity theory.

Nomenclature

C_Dh = virtual body thickness, $=2\theta$
e = hot-wire bridge voltage
h = nozzle exit height, 10.32 mm
M = Mach number
P = static pressure
P_0 = stagnation pressure
Pr = Prandtl number
P_t = pitot pressure
R = gas constant; for nitrogen, $R=297$ m^2/s^{2}K (1776 ft^2/s^2°R)
Re = unit Reynolds number, $\rho U/\mu$
Re_h = Reynolds number based on nozzle exit height and conditions averaged along the edge of the wake
T = static temperature
t = wake centerline static temperature defect, $(T_{℄}-T_e)/T_e$
T_0 = stagnation temperature
T_w = nozzle wall temperature
U = mean flow velocity
W = wake centerline velocity defect, $(U_e-U_{℄})/U_e$
Y = distance from wake centerline
Y_W = distance from nozzle wall, measured perpendicular to wake centerline
Z = streamwise distance downstream of nozzle exit, mm
γ = ratio of specific heats; for nitrogen, $\gamma=1.4$
δ = nozzle wall boundary-layer thickness
η = Howarth-Dorodnitzyn transformed lateral distance from wake centerline, $\eta=\dfrac{4W}{C_Dh}\displaystyle\int_0^Y \frac{\rho}{\rho_e}\,dy$
θ = wake momentum defect,

$$\theta=\int_{Y=-\infty}^{+\infty}\frac{\rho U}{\rho_e U_e}\left(1-\frac{U}{U_e}\right)dy$$

μ = viscosity
ρ = static density
τ = wake centerline density defect, $(\rho_e-\rho_{℄})/\rho_e$

Subscripts

℄ = conditions on the wake centerline
e = conditions at the edge of the wake or boundary layer
m = mean-flow (time-averaged) measurement
rms = root-mean-square measurement

Introduction

THE gasdynamic laser[1] (GDL) is a device capable of producing very high power levels in a continuous laser beam. A vibrationally excited mixture of N_2, CO_2, and H_2O is produced in a combustion chamber and is expanded rapidly through an array of very small two-dimensional supersonic nozzles. The rapid expansion causes a population inversion in the excited vibrational energy states of CO_2. The energy stored in this nonequilibrium gas mixture is used to amplify a probe laser beam passing through the laser cavity.

Improvements in GDL efficiency and beam quality require a detailed understanding of the fluid mechanical properties of the wakes downstream of the nozzle array. This is because the wakes extend into the laser cavity and can affect the optical properties and power level of the output laser beam. Most measurements in actual GDLs have been concerned with total laser output power and not with observations of the flowfield properties that can affect output power. Detailed wake flowfield data are extremely difficult to obtain due to limited run times and the high-temperature test environment. The purpose of this program is to examine the fluid mechanics of gasdynamic laser nozzle wakes in a model experiment where complications caused by chemical reactions and high temperatures are absent. The elimination of combustion effects from this model experiment should not be construed to imply that combustion has no effect upon the fluid mechanics of the wake. This cold-flow experiment is a simplified model relative to an actual GDL, but it is a first step in providing some

Presented as Paper 78-1214 at the AIAA 11th Fluid and Plasma Dynamics Conference, Seattle, Wash., July 10-12, 1978; submitted Sept. 25, 1978; revision received March 16, 1979.

Index categories: Lasers; Jets, Wakes, and Viscid-Inviscid Flow Interactions; Viscous Nonboundary-Layer Flows.

*Aerodynamics Department. Associate Fellow AIAA.

approximate data for evaluating theoretical GDL wake models until detailed flowfield measurements can be made in a combusting GDL.

Measurements of gasdynamic laser nozzle wake properties in noncombusting model flows are scarce. Komar and Petrie[2] measured vibrational and rotational temperatures, density, and pitot pressure profiles behind coplanar supersonic nozzles using the electron beam and pitot probes. Data were acquired in the mixing layers downsteam of these nozzles with and without gas injection into the mixing layers. Demetriades[3] conducted GDL wake studies under adiabatic wall conditions in air. Pitot pressure, stagnation temperature, and qualitative hot-wire fluctuation measurements were made in a laminar wake. In both of these experiments, the nozzles used to generate the wake flows were similar to GDL nozzles in shape, but were ten or fifteen times larger than the actual nozzles. Director[4] has made interferometer measurements of density disturbances in approximately true-scale nozzles and nozzles which were four times larger than true scale. Nearly all other studies have been limited to Schlieren photographs.

The present experiment was conceived in response to the obvious need for additional data with which to improve analytic and computer models of gasdynamic laser wakes and to insure that all important features of the wake flow are included in the models. Actual gasdynamic laser nozzles were used in this experiment to minimize the differences between these model wake flows and actual GDL wakes. Transverse pitot pressure surveys were made at twelve streamwise wake stations to define the wake boundary conditions and to identify any inviscid flow features (such as shock waves) that might affect laser performance. A complete description of the wake centerline mean-flow properties was obtained using independent measurements of pitot pressure, static pressure, and stagnation temperature. Redundant static pressure measurements using different probe geometries were made to identify any measurement errors caused by the extremely small dimensional scales of the wake. Hot-wire fluctuation measurements were used to determine whether the wakes were laminar, transitional, or turbulent. Surveys of the nozzle wall boundary layer and the inviscid flow upstream of the nozzle exit plane were made to define the initial conditions to the wake. Data were taken at two Reynolds numbers to evaluate existing linearized transitional and turbulent wake similarity theories. These measurements comprise a complete set of GDL flowfield information that can be used as a simplified, noncombusting test case for checking wake flow prediction computer codes. Details of experimental techniques, wake survey results, and comparisons of data with theory are presented.

Description of the Experiment

Three gasdynamic laser nozzles were borrowed from a prototype GDL located at Kirtland Air Force Base, Albuquerque, New Mexico, and mounted in a small open-jet wind tunnel at Sandia Laboratories. A sketch of the nozzle installation is shown in Fig. 1. Only three GDL nozzles were used in this experiment due to limitations on wind-tunnel size, the maximum available mass flow rate, and nozzle availability. Wake surveys were made downstream of nozzle 2 using probes mounted on a two-degree-of-freedom traversing mechanism.

A potential problem with the three-nozzle configuration used in this experiment is the asymmetric boundary-layer growth on the nozzles in the stagnation chamber upstream of the nozzle throats. Boundary layers are formed on the nozzle array mounting chamber and pass onto nozzles 1 and 3, but not onto nozzle 2. The thickness of the boundary layers on nozzles 1 and 3 is therefore greater than the thickness of the boundary layers growing on nozzle 2. It was feared that these differences in boundary-layer thickness could cause asymmetries in the wake and inviscid flows downstream of the nozzle exit plane. To evaluate this potential problem, provision was made to bleed the mounting chamber boundary layers through a narrow gap between the mounting chamber walls and nozzles 1 and 3. Surveys of both the wake and inviscid flowfields downstream of the nozzle array were made with and without the boundary-layer bleed activated, and no differences in flow properties were observed. Final survey data were obtained with no boundary-layer bleed in order to minimize the nitrogen mass flow rate.

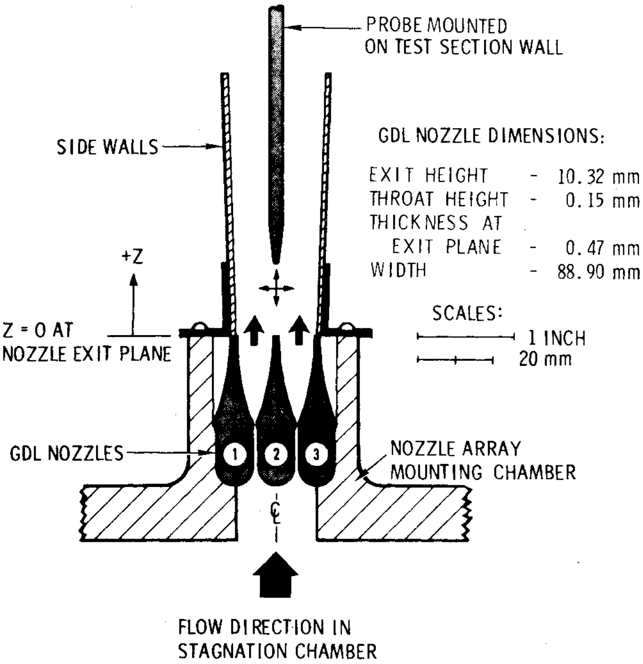

Fig. 1 Cross-sectional view of the GDL nozzle array.

Side walls were installed to simulate the presence of adjacent nozzles in actual GDL arrays. Without the side walls, shock waves were generated above nozzles 1 and 3 by the high back-pressure in the test chamber; these shocks distorted the wake flowfield to the extent that this model experiment did not simulate actual GDL wakes. The angle of the side walls relative to the wake centerline was adjusted so that pitot pressure surveys showed uniform flow across the nozzle exit plane. The side wall angle used in this experiment (1 deg outward flare) produced neither shock waves nor expansion fans in the inviscid flow along the entire length of the wake survey region (0-76 mm downstream of the nozzle exit plane).

Laminar wakes were not studied in this experiment because Ref. 3 claims successful experimental verification of the key assumptions of the laminar theory, although some disparity between the quantitative predictions of the laminar theory and laminar wake data was observed. Furthermore, the normal operating Reynolds number range of combusting gasdynamic lasers is high enough to generate transitional and turbulent wakes. Test conditions for this experiment were selected to generate transitional and turbulent wake flows for these reasons. Reynolds numbers (based on nozzle exit height and nominal wake edge conditions) of 220,000 and 42,600 were achieved by operating the facility at $P_0 = 1593$ kN/m^2, $T_0 = 398$ K and $P_0 = 212$ kN/m^2, $T_0 = 285$ K, respectively, using pure nitrogen as the test gas. The nominal Mach number at the edge of the wake was 5.71 for $Re_h = 220{,}000$ and 5.97 for $Re_h = 42{,}600$; Fig. 2 shows the variation of edge Mach number as a function of distance downstream of the nozzle exit plane at both test Reynolds numbers. The nozzles were operated at adiabatic wall temperature for both test conditions. Pitot pressure measurements verified that the time-averaged wake behind the center nozzle was two-dimensional.

Static temperatures at the edge of the wake are 35 K at $Re_h = 42{,}600$ and 53 K at $Re_h = 220{,}000$. The flow is supersaturated in both cases. Detailed wake surveys were made at

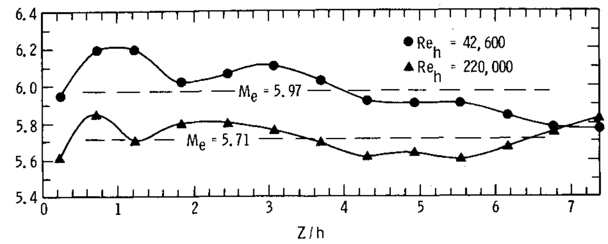

Fig. 2 GDL wake edge Mach number distribution.

higher temperatures (above the condensation temperature) and at lower temperatures to see whether supersaturation affected the wake data presented in this paper. No differences in flow properties were observed between surveys conducted at the supersaturated temperatures reported in the text and the surveys conducted at temperatures above the condensation limit. Supersaturation effects were not observed until the static temperature was lowered to between 46 K and 38 K at the higher Reynolds number test condition. The temperature range at which supersaturation effects appeared agrees well with the empirical data presented by Daum and Gyarmathy.[5]

Flowfield Instrumentation

Pitot Probes

Pitot pressure measurements were made across the nozzle wall boundary layer at four stations upstream of the nozzle exit and across the viscous and inviscid wake at twelve stations downstream of the nozzle exit. The extremely small dimensional scales of the wake required special probe configurations, data validation procedures, and corrections to the measurements. Flat-tipped pitot probes were used to increase the response time of the probe while minimizing the external size of the probe tip relative to the wake width. In order to eliminate probe interference effects, the height of the probe tip was reduced until no differences in the measured pitot pressures could be observed between the smallest probe and the next larger probe. The pitot probe used in this study had a tip height of 0.38 mm and a tip width of 1.27 mm, as shown in Fig. 3a. The small tip size and low unit Reynolds numbers on the wake centerline made it necessary to correct centerline pitot pressure measurements for viscous effects using the correlation of Ref. 6.

Static Probes

Wake centerline static pressures were measured using two different static probe geometries. The larger of these configurations was a conventional cone-cylinder probe with two 0.74-mm-diam orifices located on the wake axis on either side of the cylinder. Figure 3b is a sketch of the large static probe. Due to the length of the portion of the probe in front of the orifices, this probe could only be used at wake survey locations downstream of $Z/h = 1.85$. Viscous interaction corrections to measured static pressures were made following Ref. 6. The maximum correction was less than 2% of the measured value.

The diameter of the large static probe was 1.09 mm, which is approximately one-quarter of the wake width at the high Reynolds number test condition. Since this probe diameter was larger than is desired to insure interference-free static pressure data, five smaller static probes were constructed (Fig. 3c) to check the larger probe results. The diameter of the small probes was made nearly equal to the width of the flat base on the GDL nozzles. The usual static probe conical tip was eliminated in favor of a flat tip so that each probe could be butted up against the nozzle base. The flow from the GDL nozzles passed smoothly onto the static probe without encountering any shock waves at the probe tip. This probe configuration made viscous interaction corrections unnecessary and reduced probe/flow interactions to a minimum. Another advantage of the small static probe configuration was that measurements could be made closer to the nozzle exit plane than measurements using the larger static probe. Each of the five probes in Fig. 3c was designed to provide data at a different distance Z downstream of the nozzle exit. The only problems encountered with these probes were associated with the slow pressure response time due to the 0.08-mm-diam pressure orifices. Special measurement techniques and calibration procedures had to be developed for these probes, and 30-min run times were needed to obtain a single steady-state pressure data point.

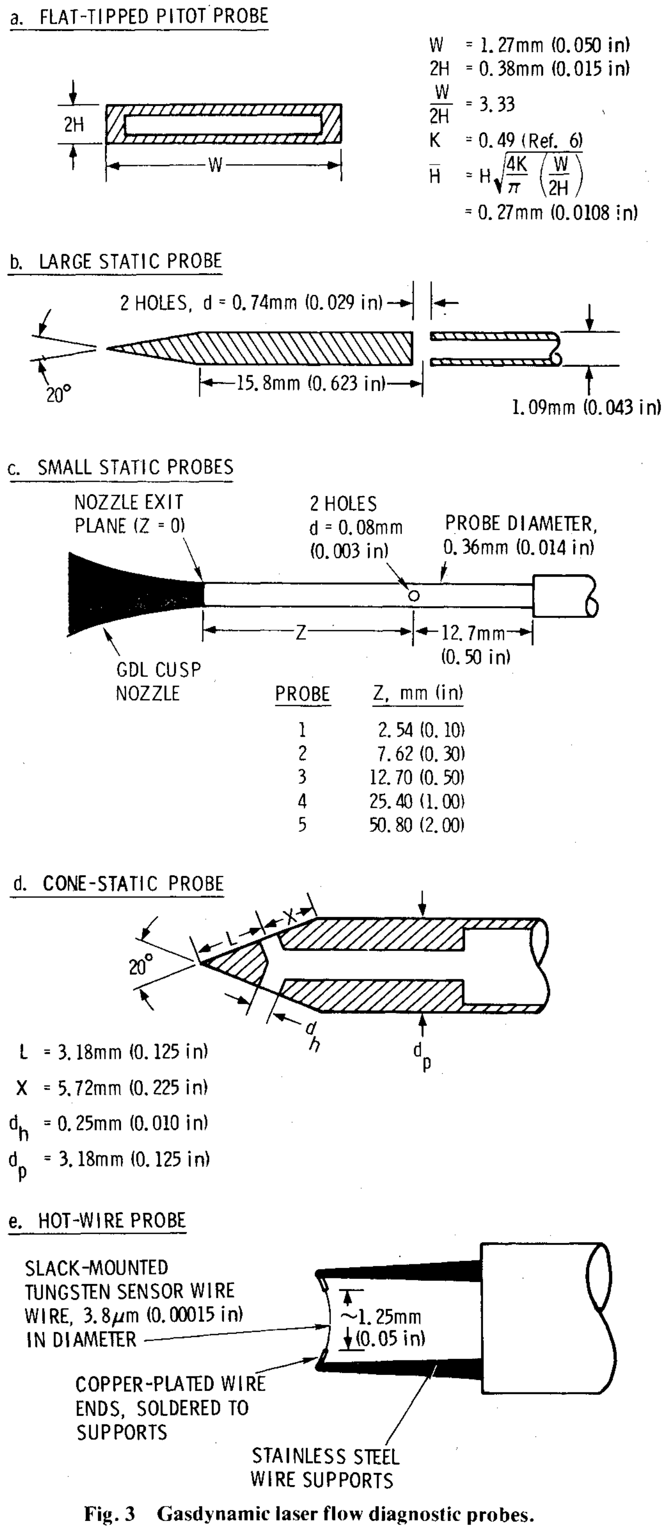

Fig. 3 Gasdynamic laser flow diagnostic probes.

Cone-Static Probe

A 10-deg half-angle cone-static pressure probe was used in addition to the static pressure probes to determine flowfield properties on the wake centerline. This probe, shown in Fig. 3d, has pressure orifices much closer to the tip of the probe (3.18 mm) than the static probes. This feature was believed to be advantageous because it can minimize measurement errors due to axial and lateral pressure gradients. The probe was considerably larger in diameter than either of the static probes and occupied more than half of the wake width. The large probe diameter was necessary to make the X dimension on Fig. 3d large enough to eliminate measurement errors caused by the upstream influence of the cone shoulder expansion fan. Although the overall diameter of the cone-static probe is large, the diameter of the probe at the pressure ports (where the measurement is made) is comparable to the diameter of the larger static probe. For this reason, the cone-static probe was not disqualified a priori from consideration as a wake diagnostic technique for this experiment. Reference 6 was used to correct cone-static probe data for viscous interaction effects. Maximum corrections were less than 5% of the measured value.

Hot-Wire Probe

Stagnation temperatures and turbulent fluctuations were measured using a DISA 55D01 constant temperature anemometer and a Thermo-Systems tungsten hot-wire probe. Tungsten was used as the wire material because it is very strong and is commercially available in smaller diameters than most other wire materials. A sensor wire diameter of 3.8 μm was selected to maximize frequency response. A conventional square-wave test conducted in the inviscid flow region at an overheat ratio of 0.8 established the hot-wire system maximum frequency response at approximately 150 kHz. The wire was mounted with some slack on the steel supports to eliminate strain gage effects. Figure 3e is a sketch of the hot-wire probe.

Quantitative stagnation temperature data were obtained by operating the wire at zero overheat ratio and measuring the wire resistance. The relationship between wire resistance and wire recovery temperature was determined by calibration at known stagnation temperatures in the inviscid nozzle flowfield. Reference 7 was used to calculate centerline stagnation temperature from measured wire recovery temperature. An iterative data reduction computer program was used to make this temperature correction as well as all pressure probe corrections.

Quantitative information on fluctuating flow properties was not obtained in this study because the constant temperature anemometer places severe restrictions on hot-wire frequency response at the low overheat ratios needed to obtain complete modal diagrams. Instead, rms bridge voltages were measured in the viscous wake at an overheat ratio of 0.8 to identify qualitatively the regions of laminar, transitional, and turbulent flow in the wake.

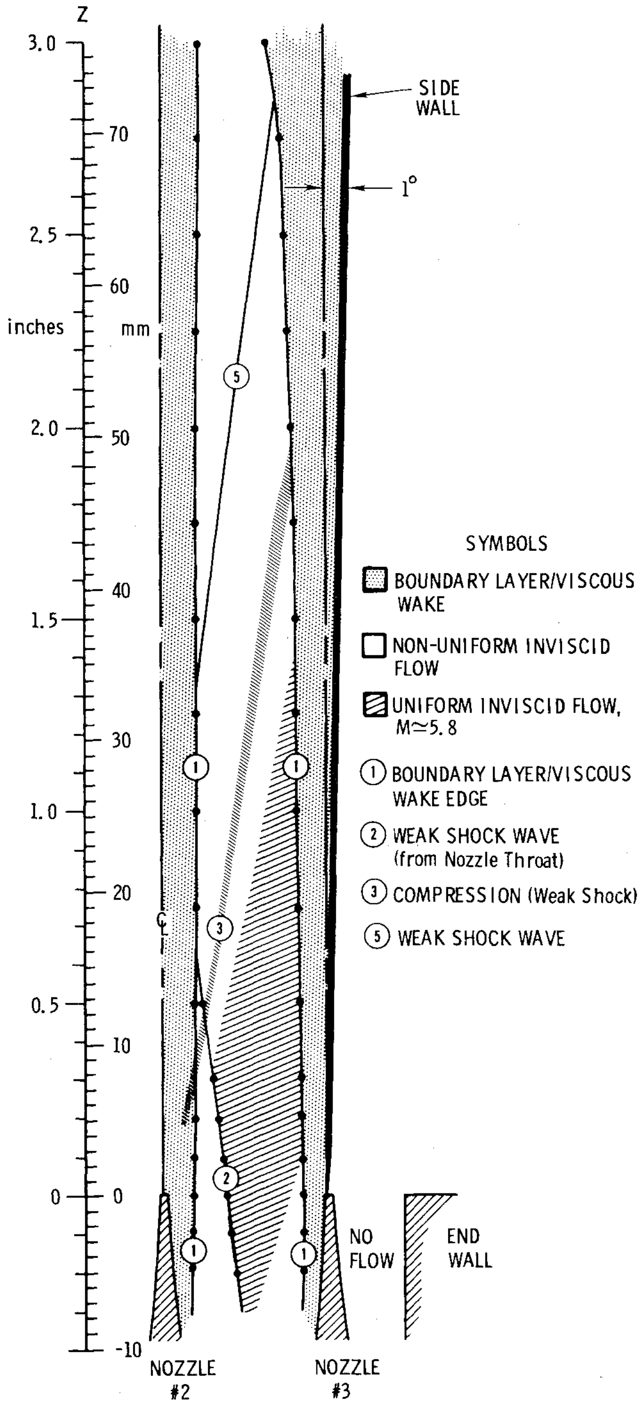

Fig. 4 GDL flowfield map, $Re_h = 42{,}600$.

Evaluation of Probe Interference Measurement Errors

The use of intrusive flow diagnostic techniques in small-scale laser wakes required that an assessment of probe interference errors be made before drawing any conclusions about the fluid mechanics of the wake. Probe interference errors were evaluated by making redundant static probe measurements on the wake centerline, using the cone-static probe and the two static probe configurations. Data from each of these probes were combined with pitot pressure and stagnation temperature to calculate Mach number along the wake centerline. By comparing these Mach number distributions, it was anticipated that any errors due to the specific geometry of the probe could be identified. Identification of erroneous data should not be difficult because the geometries and sizes of these three probes are so different from one another. Since the magnitude of probe interference effects depends primarily on probe geometry and size, it can be safely assumed that the extent of interference errors, if any, will be significantly different for each probe.

Centerline Mach number distributions calculated from the three different static probe configurations agreed closely at $Re_h = 220{,}000$. At $Re_h = 42{,}600$, Mach number data from the two static probes were identical, but cone-static probe Mach numbers were lower than either static probe Mach numbers along the entire wake axis. It was concluded that the cone-static probe suffers from small probe interference errors at $Re_h = 42{,}600$. Final wake centerline data were obtained by using only the static probe results, which appear to be free from interference effects because of their excellent agreement at both Reynolds numbers.

Gasdynamic Laser Flowfield Map

Pitot surveys upstream and downstream of the nozzle exit were used to construct a map of the gasdynamic laser flowfield (Fig. 4). Of particular interest are the weak shock waves which traverse the laser cavity. Wave 3 originates near the trailing edge of the center GDL nozzle and is similar to the wake shock observed behind re-entry vehicles. Wave 2 emanates from the outer nozzles near the throat and propagates into the viscous wake near $Z=15$ mm. It is caused by very small (~ 0.03 mm) misalignments of the GDL nozzle cusp throats. Wave 5 is a continuation of wave 2 after it emerges from the viscous wake. Although wave 2 could have been eliminated by realignment of the center nozzle, it was decided to conduct the experiment with wave 2 as shown because similar alignment errors (with similar shock waves) can be expected in actual combusting gasdynamic lasers.

It is important to assess the strength of any waves which pass through the viscous wake because these waves have the potential to degrade the performance of an actual GDL. The angles of waves 2, 3, and 5 relative to the inviscid nozzle flow are approximately the same as the angle of a Mach wave, indicating that these waves are nearly isentropic. Furthermore, none of these waves causes any major changes in the width of the viscous wake, as can be seen in Fig. 4. No significant degradation of laser output power would occur if waves of similar strength traversed the optical cavity of a combusting GDL.

Even though these waves are weak, they may nevertheless introduce pressure gradients in the wake which, in turn, may change other wake flowfield properties in ways which are not taken into account by existing theoretical models. Figure 5 presents the streamwise static pressure distributions on the wake centerline and at the wake edge for $Re_h=42{,}600$ and $Re_h=220{,}000$. There is no indication of large discontinuities in either the centerline or the edge static pressure distributions, which is further evidence that waves 2, 3, and 5 are not strong shocks. The continuous variation of static pressure along the wake indicates that waves 2, 3, and 5 are part of a more extensive system of compression and expansion waves that pass through the viscous wake along the entire region surveyed. Some of these waves emanate from the GDL nozzles; they are caused by the nozzle misalignment and the fact that the test gas has a different ratio of specific heats than the N_2-CO_2-H_2O gas mixture for which the nozzles were designed. The effects of the wake pressure gradients upon other measured wake properties and their comparisons with theory are discussed in subsequent sections.

Hot-Wire Turbulence Measurements

To determine the laminar/transitional/turbulent status of these wakes, qualitative hot-wire fluctuation measurements

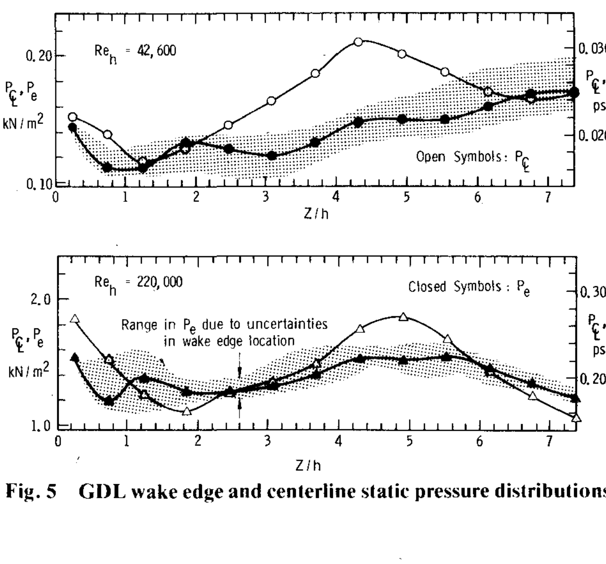

Fig. 5 GDL wake edge and centerline static pressure distributions.

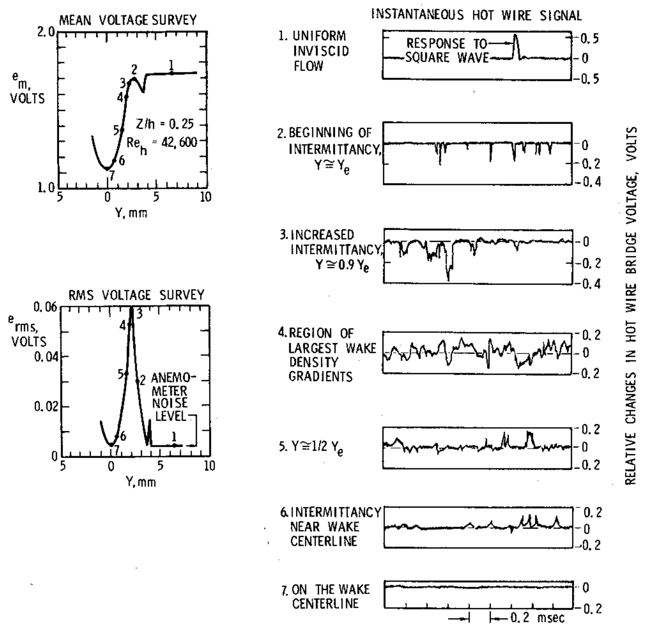

Fig. 6 Hot-wire survey across the GDL wake, $Re_h=42{,}600$.

were made across the wake at two survey stations and at both test conditions. Figure 6 shows the results of a hot-wire survey made at $Z/h=0.25$ for $Re_h=42{,}600$. The mean voltage survey looks very much like the pitot pressure survey, which is to be expected, since both the hot-wire and the pitot probe respond primarily to changes in density across the wake. Root-mean-square hot-wire measurements show that significant fluctuations exist near the outer edge of the wake, but the rms hot-wire signal vanishes on the wake centerline. Hot-wire surveys at $Z/h=7.38$ followed the same trend: fluctuations were observed only near the edge of the wake and not on the wake centerline. It was concluded from these measurements that the wake is transitional at $Re_h=42{,}600$, with the turbulence confined to the region near the edge of the viscous wake.

A comparison of the unit Reynolds number on the wake centerline with the unit Reynolds number at the edge of the wake provides an explanation of why turbulent fluctuations appear near the wake edge but not on the wake centerline at $Z/h=0.25$ and $Re_h=42{,}600$. Using measurements of centerline pitot pressure, static pressure, and stagnation temperature, the values of wake centerline velocity and density are calculated as follows:

$$P_{℄}=152\ \mathrm{N/m^2}\ (0.0220\ \mathrm{psia}),\quad T_{℄}=207\ \mathrm{K}\ (373.3°\mathrm{R})$$

$$M_{℄}=0.976,\ U_{℄}=M_{℄}\sqrt{\gamma R T_{℄}}=287\,\mathrm{m/s}\ (940\,\mathrm{ft/s})$$

$$\rho_{℄}=P_{℄}/RT_{℄}=0.246\times 10^{-2}\ \mathrm{kg/m^3}\ (0.478\times 10^{-5}\ \mathrm{slugs/ft^3})$$

The Sutherland viscosity relation[8] is used for temperatures above 180°R:

$$\mu_{℄}=2.1996\times 10^{-8}T_{℄}/1+\frac{201.6}{T_{℄}}=1.32\times 10^{-5}\ \mathrm{N\cdot s/m^2}$$

$$=2.75\times 10^{-7}\ \mathrm{slugs/ft\ s}$$

The unit Reynolds number on the wake centerline is:

$$Re_{℄}\equiv\rho_{℄}U_{℄}/\mu_{℄}=5.33\times 10^{4}\ \mathrm{m^{-1}}\ (1.62\times 10^{4}\ \mathrm{ft^{-1}}) \quad (1)$$

Calculation of unit Reynolds number at the wake edge proceeds in the same manner, using measured values of wake edge flow properties:

$$P_e = 143 \text{ N/m}^2 \ (0.0207 \text{ psia}),\ T_e = 35 \text{ K } (63.6°\text{R})$$

$$M_e = 5.944,\ U_e = M_e\sqrt{\gamma R T_e} = 721 \text{ m/s } (2364 \text{ ft/s})$$

$$\rho_e = P_e / R T_e = 1.36\times 10^{-2} \text{ kg/m}^3 \ (2.638\times 10^{-5} \text{ slugs/ft}^3)$$

A linear viscosity relationship[8] is used for temperatures below 180°R:

$$\mu_e = 7.733491\times 10^{-10}\times T_e = 0.23\times 10^{-5} \text{ N}\cdot\text{s/m}^2$$

$$= 0.49\times 10^{-7} \text{ slugs/ft s}$$

The unit Reynolds number at the wake edge is:

$$Re_e \equiv \rho_e U_e / \mu_e = 4.18\times 10^6 \text{ m}^{-1} (1.27\times 10^6 \text{ ft}^{-1}) \qquad (2)$$

The calculations show that the unit Reynolds number at the wake edge is nearly eighty times larger than the unit Reynolds number on the wake centerline at $Z/h = 0.25$. At downstream wake locations, the ratio $Re_e / Re_{\mathbf{\text{℄}}}$ decreases because the wake centerline velocity increases, the centerline temperature (and viscosity) decreases, and the centerline density increases while the wake edge conditions remain about the same. Nevertheless, the unit Reynolds number on the wake centerline is more than an order of magnitude smaller than the wake edge unit Reynolds number at all streamwise survey stations. For $Re_h = 42{,}600$, the unit Reynolds number near the edge of the wake is high enough to sustain the turbulence generated in the wake shear layer, but the unit Reynolds number on the wake centerline is too low to allow turbulence to exist.

When the GDL operating Reynolds number was increased above 42,600, the transitional/turbulent region extended closer to the wake centerline. At $Re_h = 220{,}000$ and both survey stations, fluctuations were observed everywhere in the wake, including the wake centerline. The wake was judged to be turbulent at this Reynolds number, based upon the extent and frequency of the hot-wire fluctuation data.

Observations of the transitional and turbulent status of the GDL wake were compared to predictions by Demetriades,[9] who uses a technique based upon a postulated minimum turbulence Reynolds number required to sustain turbulence once it occurs. For $Re_h = 42{,}600$, Ref. 9 predicts that the wake is completely laminar at all streamwise survey stations. For $Re_h = 220{,}000$, transition is predicted at $Z/h = 2.5$ (50 mm downstream of the nozzle throat). It is possible that the small nozzle misalignment or the boundary layer growing on the subsonic region of the GDL nozzles may be partially responsible for the discrepancy between these predictions and experimental data. Reference 9 also reports a discrepancy between experimental results and predictions of transition onset. It is suggested in this reference that the discrepancy could be caused by an erroneous prediction of laminar $C_D h$ at the trailing edge of the GDL nozzle; perhaps errors in calculated $C_D h$ cause the differences between experiment and theory in the present experiment. Additional flowfield measurements are needed to determine whether any of these postulated explanations are correct. The adverse pressure gradients in the wake are definitely not responsible for the early appearance of transition, since transition is observed upstream of the region where adverse pressure gradients exist.

Nozzle Exit Plane Boundary-Layer Surveys

Figure 7 presents the pitot pressure, velocity, density, and static temperature profiles across the GDL nozzle boundary layer at the nozzle exit plane ($Z/h = 0.0$) for both the high and low Reynolds number test conditions. Boundary-layer profiles were obtained by combining measured pitot pressure surveys with assumptions on the transverse static pressure distribution (constant across the boundary layer) and the stagnation temperature distribution (wake measurements at $Z/h = 0.25$ were used to estimate the profile shape and magnitude). The strong dependence of profile shape upon Reynolds number is consistent with the results of wake hot-wire turbulence measurements discussed in the preceding section. The "full" velocity and density profiles observed at $Re_h = 220{,}000$ suggest a fully-developed turbulent boundary layer, and the "less full" profiles at $Re_h = 42{,}600$ are characteristic of a transitional boundary layer. These boundary-layer profiles represent the initial conditions to the wake flow.

Discussion of Wake Measurements

Final gasdynamic laser wake centerline static pressure and Mach number distributions for both test Reynolds numbers are shown in Figs. 5 and 8. Also shown on these figures are the ranges of static pressures and Mach numbers obtained by assuming that the centerline static pressure is equal to the static pressure at the edge of the wake. At some survey stations, it was sometimes difficult to determine precisely the wake edge location from lateral pitot pressure surveys due to the weak pressure waves which pass through the wake. Shaded areas are used in these figures to indicate the range of possible centerline static pressures and Mach numbers resulting from the assumption $P_{\text{℄}} = P_e$ and the uncertainties in the value of Y_e from which values of P_e are obtained. The best values of Y_e (and P_e) were determined using both pitot pressure and total temperature lateral surveys. Figure 5 shows

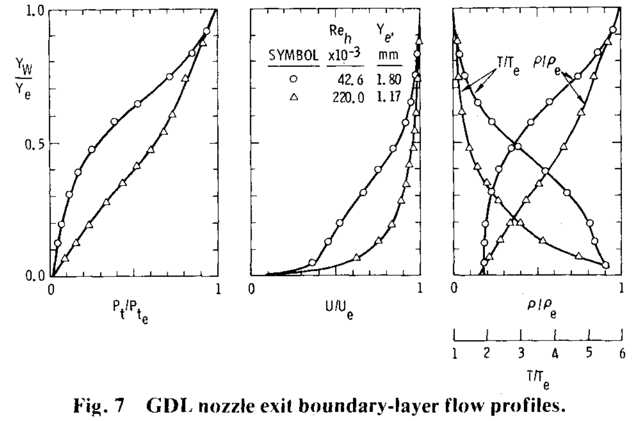

Fig. 7 GDL nozzle exit boundary-layer flow profiles.

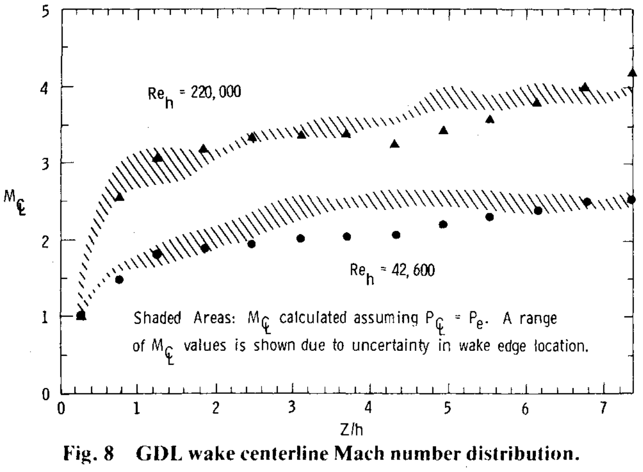

Fig. 8 GDL wake centerline Mach number distribution.

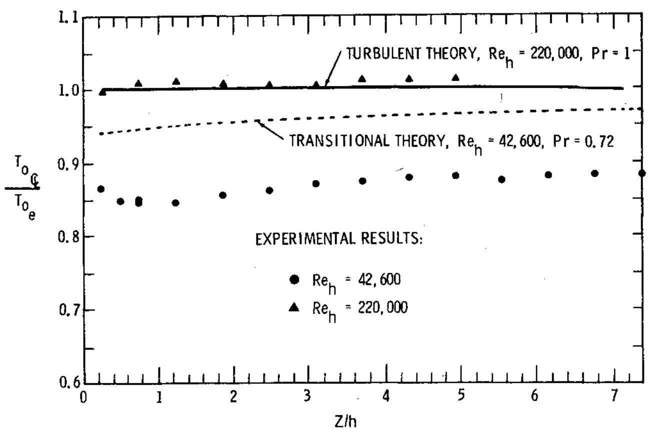

Fig. 9 GDL wake centerline stagnation temperature distribution.

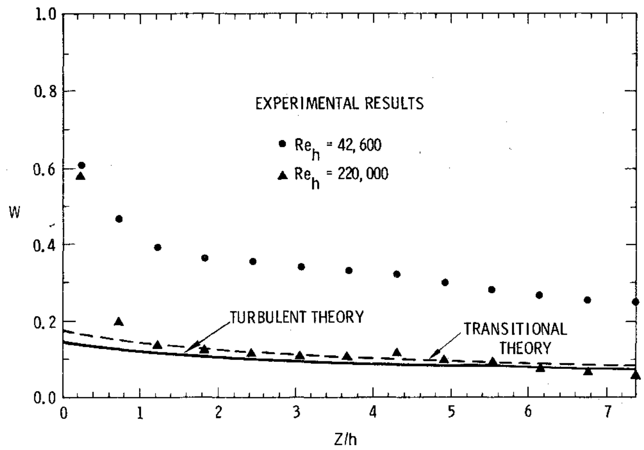

Fig. 10 GDL wake centerline velocity defect.

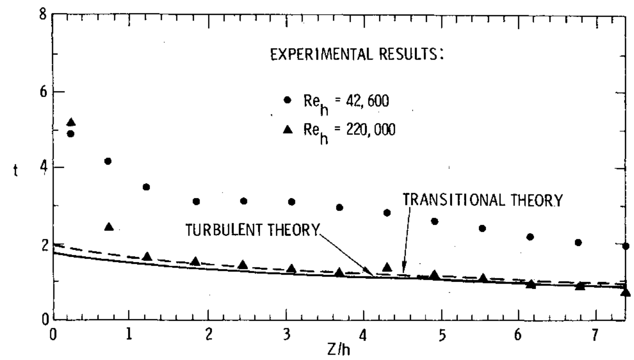

Fig. 11 GDL wake centerline static temperature defect.

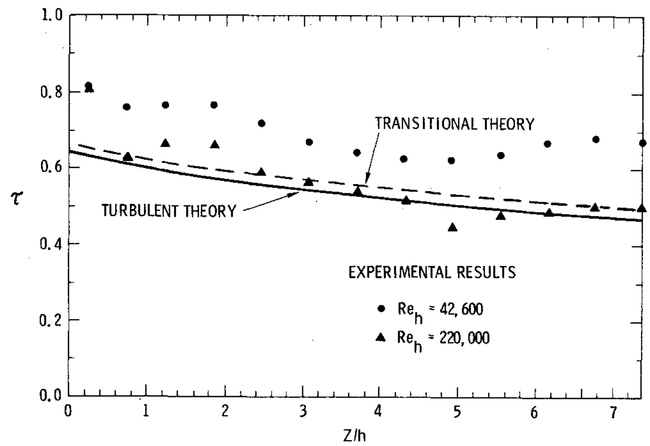

Fig. 12 GDL wake centerline density defect.

that measured wake centerline static pressures can be as much as 40% above the edge static pressure. Theoretical and numerical treatments of GDL wakes assume no difference between edge and centerline static pressure. Figure 8 indicates the magnitude of the errors in Mach number which would be encountered if the assumption $P_{\mathbb{C}} = P_e$ were substituted for static pressure measurements everywhere along the wake centerline.

Theoretical predictions of laminar, transitional, and turbulent GDL wakes have been proposed by Demetriades in Refs. 9 and 10. Demetriades' theories relate centerline flow properties and lateral flow profiles to the wake momentum defect and heat transferred to the flow from the nozzles. Kubota's[11] linearized ($W \ll 1$) similarity solutions for laminar compressible wakes form the basis for Demetriades' analyses. An analytic expression for velocity defect is used for laminar wakes,[10] but the expression for W in turbulent wakes is assumed[10] and turbulent transport coefficient values are taken from experiment.[12] Demetriades' treatment of transitional wakes[9] assumes a laminar nozzle wall boundary layer, a turbulent wake, and transition located everywhere across the wake at the nozzle exit plane ($Z/h = 0.0$).

Experimental values of turbulent wake centerline total temperature, velocity defect, static temperature defect, and density defect are compared to Demetriades' turbulent wake predictions in Figs. 9-12. Inputs for these theoretical turbulent wake calculations were $M_e = 5.71$, $Re_h = 220{,}000$, $Pr = 1.0$, and $T_w/T_0 = 1.0$. Immediately downstream of the nozzle exit plane ($Z/h < 1.2$), the turbulent wake is not in equilibrium and, therefore, calculated values of W, t, and τ do not agree with measurements. Downstream of $Z/h = 1.2$, however, good agreement was observed between measured turbulent wake centerline properties and predictions of the turbulent linearized theory. The pressure gradients observed in the turbulent wake cause some scatter of the turbulent density defect data around the turbulent prediction, but the magnitude of the scatter is not large enough to detract from the accuracy of the prediction. The pressure gradients have a negligible effect on the comparison of static temperature and velocity defect data with theoretical predictions.

Inputs for transitional wake centerline predictions[9] were $M_e = 5.97$, $Re_h = 42{,}600$, $Pr = 0.72$, and $T_w/T_0 = \sqrt{Pr}$. Figures 9-12 show poor agreement between transitional wake data and transitional theory. The presence of pressure gradients in the wake cannot explain the differences between theory and experiment—even if the data are reduced using a constant static pressure corresponding to the nominal edge conditions ($M_e = 5.97$ and $P_e/P_0 = 6.53 \times 10^{-4}$) instead of measured values of $P_{\mathbb{C}}$, the transitional theory still underpredicts the transitional velocity defect data by more than 50%. Discrepancies are obtained because the model of transition assumed in the analysis is quite different from the observed development of transition in this experiment. Better agreement would require an improved model of transition, quantification of the transitional state of the wake, and the ability to calculate the wake momentum defect as a function of the transitional state.

Experimental lateral velocity, temperature, and density profiles are plotted as a function of the dimensionless lateral coordinate η for the transitional and turbulent wakes in Figs. 13 and 14. Transitional wake profile data are compared with theoretical profiles for a transitional wake. To obtain these theoretical profiles, transition is assumed to occur at the nozzle exit, the nozzle boundary layer is assumed to be laminar, and the turbulent form of lateral wake flow properties is used; this approach is identical to that used in Ref. 9 to calculate transitional wake centerline flow

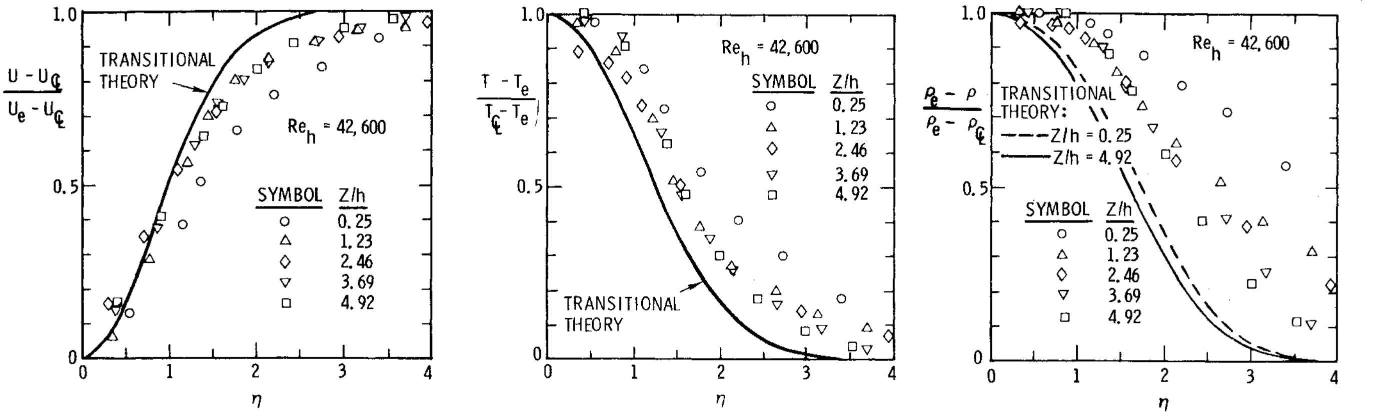

Fig. 13 GDL lateral wake profiles, $Re_h = 42{,}600$.

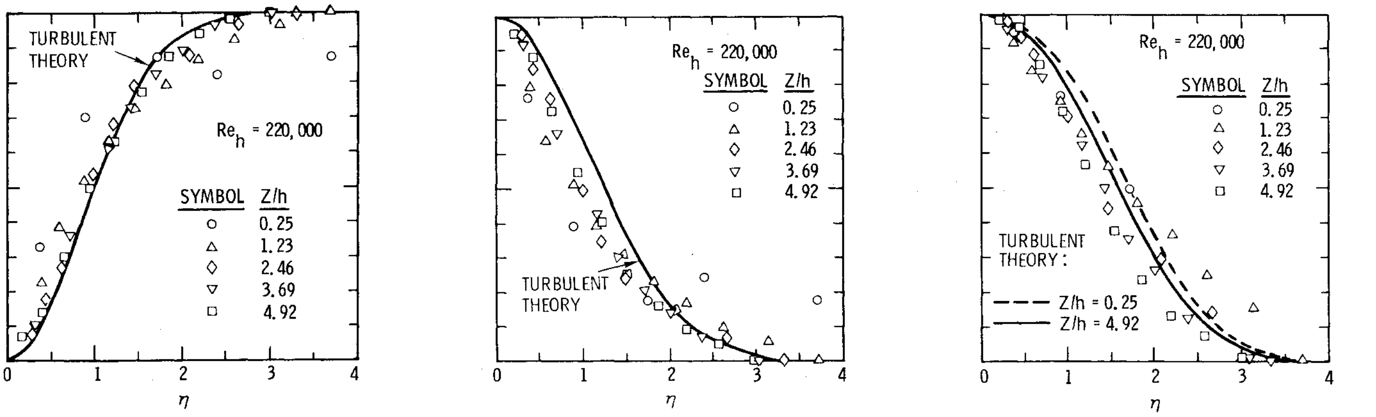

Fig. 14 GDL lateral wake profiles, $Re_h = 220{,}000$.

properties. Poor agreement between theoretical profiles and measurements are observed for this transitional wake. However, turbulent wake profile data are successfully correlated using the linearized turbulent theory at all survey stations downstream of $Z/h = 1.2$.

Summary and Conclusions

A cold-flow experiment using nozzles from an actual gasdynamic laser was conducted in an open-jet wind tunnel to provide detailed information on the fluid mechanical properties in the wakes downstream of the GDL nozzle array. Extensive mean-flow measurements and qualitative turbulence measurements were made in transitional and turbulent wakes so that analytic and numerical GDL wake flowfield prediction schemes could be evaluated. Redundant mean-flow measurements proved to be necessary to eliminate data affected by probe interference effects. Hot-wire measurements showed that the GDL wake is transitional at $Re_h = 42{,}600$. Fluctuations were observed only near the wake edge, where the local Reynolds number is high enough to sustain turbulence, and not on the wake centerline, where the Reynolds number is too low to allow turbulence to exist. Wake transition theory predicts purely laminar wakes at this value of Re_h. As Reynolds number was increased, the region of turbulence in the wake extended closer to the wake centerline. The wake was completely turbulent at $Re_h = 220{,}000$.

Transverse pitot pressure surveys indicated that shock waves are formed by very small misalignments of the nozzle throat, and that these shocks extend into the laser cavity. In this experiment, these shocks were very weak. No reductions in laser output power would occur if waves of similar strength were observed in a combusting GDL. However, these waves were part of an extensive network of compression and expansion waves which caused streamwise and lateral pressure gradients at all wake survey stations. As a result of this network, measured wake centerline static pressures were found to be as much as 40% higher than edge static pressures. This result is contrary to the assumption of no lateral pressure gradients made in all GDL wake theories. However, the pressure gradients were not an important factor in determining the success of comparisons between experimental data and predictions of a linearized GDL wake theory.

Turbulent wake centerline and lateral profile data showed good agreement with the predictions of a linearized turbulent similarity theory. However, the linearized transitional theory was not able to predict measured flow properties in the transitional wake. Major changes in the transitional wake theory, most of which are well beyond the scope of a similarity analysis, would be necessary to improve the accuracy of transitional wake predictions.

Acknowledgments

This work was supported by the Air Force Weapons Laboratory Laser Research Laboratory, Kirtland Air Force Base, New Mexico, and the U.S. Dept. of Energy. The author wishes to thank P. J. Ortwerth of the Air Force Weapons Laboratory for his comments and technical inputs to this work. In addition, the author is indebted to D. A. Powers and D. E. Berg of Sandia's Experimental Aerodynamics Division for their assistance in making the measurements described in this paper.

References

[1] Gerry, E. T., "Gasdynamic Lasers," *IEEE Spectrum*, Nov. 1970, pp. 51-58.

[2]Komar, J. J. and Petrie, S. L., "Investigation of Fluid Dynamic Interactions Within Multiple Nozzle Arrays," AIAA Paper 76-342, San Diego, Calif., July 1976.

[3]Demetriades, A., "Experimental Test of the Theory of Multiple-Nozzle Cusp Wakes," Aeronutronics Publication No. U-6395, Ford Aerospace & Communications Corp., Newport Beach, Calif., Dec. 1977.

[4]Director, M. N., "Aerodynamic Parameters Affecting Practical Gas Dynamic Laser Design," AIAA Paper 73-626, Palm Springs, Calif., July 1973.

[5]Daum, F. L. and Gyarmathy, G., "Condensation of Air and Nitrogen in Hypersonic Wind Tunnels," *AIAA Journal*, Vol. 6, March 1968, pp. 458-465.

[6]Peterson, C. W. and George, O. L., "Wind Tunnel Pressure Probes: New Calibrations for New Geometries and Flow Environments," SAND75-0337, Sandia Laboratories, Albuquerque, N. Mex., June 1975; also, *AIAA Journal*, Vol. 13, Oct. 1975, pp. 1263, 1264.

[7]Behrens, W., "Total Temperature Thermocouple Probe Based Upon Recovery Temperature of Circular Cylinder," *International Journal of Heat Mass Transfer*, Vol. 14, Oct. 1971, pp. 1621-1630.

[8]Boudreau, A.H. Jr., "High Mach Number-High Reynolds Number Perfect Gas Wind Tunnels and a Method of Performance Comparison," Arnold Engineering Development Center Rept. AEDC-TR-69-268, ARO, Inc., Jan. 1970.

[9]Demetriades, A., "Transition and Turbulence in Gas-Dynamic-Laser Nozzle Wakes," Aeronutronics Publication No. U-6328, Ford Aerospace and Communications Corp., Newport Beach, Calif., April 1977.

[10]Demetriades, A., "Linearized Analysis of Gasdynamic-Laser Wakes with Applications," *Journal of Energy*, Vol. 1, March-April 1977, pp. 73, 74.

[11]Kubota, T., "Laminar Wakes with Streamwise Pressure Gradient," GALCIT Hypersonic Research Project IM No. 9, California Institute of Technology, Pasadena, Calif., May 1962.

[12]Demetriades, A., "Turbulent Mean-Flow Measurements in a Two-Dimensional Supersonic Wake," *The Physics of Fluids*, Vol. 12, Jan. 1969, pp. 24-32.